Proceedings of the 11th Brazilian Congress of Thermal Sciences and Engineering -- ENCIT 2006
Braz. Soc. of Mechanical Sciences and Engineering -- ABCM, Curitiba, Brazil,- Dec. 5-8, 2006

Paper CIT06-864

NUMERICAL SIMULATION OF THE LAMINAR FLOW AROUND A CIRCULAR CYLINDER WITH STREAM-WISE HARMONIC OSCILLATION

Daniel Martins da Silva
Departamento de Engenharia Mecânica, Faculdade de Tecnologia, Universidade de Brasília, Campus Universitário Darcy Ribeiro, 70910-900, Brasília, DF, Brasil
danielunb@pop.com.br

Roberto Francisco Boberieth Miserda
Departamento de Engenharia Mecânica, Faculdade de Tecnologia, Universidade de Brasília, Campus Universitário Darcy Ribeiro, 70910-900, Brasília, DF, Brasil
rfbm@unb.br

Abstract. *The objective of the present study is the numerical simulation of the two-dimensional laminar flow around a circular cylinder that oscillates harmonically in the stream-wise direction. The problem is solved for a non-inertial frame of reference that is moving with the cylinder and, for this reason, the associated pseudo-force and pseudo-work terms are included as sources in the compressible Navier-Stokes equations. These equations are solved using a finite volume formulation, where the fluxes are calculated using the fourth-order skew-symmetric form of Ducros' algorithm, while the time marching is achieved using the third-order Runge- Kutta scheme proposed by Shu. For all cases studied, the Reynolds number is 100 and the Mach number is 0,20. In the present work, the impact over the flow topology of two parameters is analyzed. The first one is the maximum linear velocity of the oscillating cylinder and the second one is the frequency of the harmonic oscillation. Depending on the combinations of these parameters the structure of the wake presents three distinct forms: (i) periodic and symmetric, where a symmetric vortex pair is emitted in each cycle of oscillation resulting in a null normal force; (ii) periodic and anti-symmetrical, resulting in a superposition of the previous mode over the von Kármán vortex street and (iii) chaotic, where the vortex systems are emitted with no regularity in each cycle of oscillation.*

Keywords: *Numerical simulation, stream-wise oscillation, wake topology, laminar flow, dynamic systems.*

1. Introduction

Usually, when vortices inducing oscillations on rigid bodies are mentioned the primordial thought is of a cylinder oscillating in the normal direction of the flow, since the emission of vortices for a compressible flow produces periodic forces that act primordially in the transversal direction of the flow. The component in the parallel direction of the flow has frequency next to two times the frequency of emission of vortices, number of Strouhal (*St*), and typically its magnitude is less than the component in the normal direction and incapable to excite the structure. The Strouhal number is a dimensionless parameter that represents the frequency with which consecutive vortices of same signal are emitted and is defined as $St = f\ D/U_\infty$, where f represents the characteristic frequency of emission of vortices, D represents the characteristic length of the system and U_∞ indicates the velocity of the non-disturbed region. In this context, one of the pioneers in the experimental analysis for this configuration of the flow was Griffin and Ramberg (1976), it was evidenced that the flow submitted to harmonic oscillations depends strongly on the Keulegan-Carpenter, KC, nondimensional number that represents the relation between the frequencies of oscillation by the convective time scale. Was noticed that to the measure that KC increases, remaining constant the Reynolds number, the format of the emitted vortices was modified. Tastsuno & Bearman (1990), in an experimental work and based in visualization, describe the several regimes.

Under purpose of the present research project, Öngoren & Rockwell (1988), had carried through extensive experiments on the forced oscillation of an in-line circular cylinder with the incident flow, two basic modes of emission of vortices had been observed, the symmetrical form and the anti-symmetrical form, this last one with four possible configurations as shown in Fig. 01, in which modes A-III and A-IV only occur when the cylinder describes a harmonic oscillation, they had evidenced that the dominant model of emission of vortices is the symmetrical case, observed in Fig. 1(a). Öngoren & Rockwell (1988), had noticed that initially when the cylinder describes a sine movement, have a transient emission of vortices that is characterized by the symmetrical mode, which decay gradual for the anti-symmetrical mode, however, it's possible for certain configuration of the parameters to have the steady symmetrical form. In general lines, they had concluded that the excitement of the cylinder in the direction of the flow generates symmetrical disturbances, while the natural and predominant occurrence in the normal direction generates anti-symmetrical disturbances. Consequently, it will have competitions between the phenomena, symmetrical and anti-symmetrical mode, consequently under certain conditions one in the modes it will prevail, producing the synchronization it enters the structure of the flow near to the cylinder and its movement.

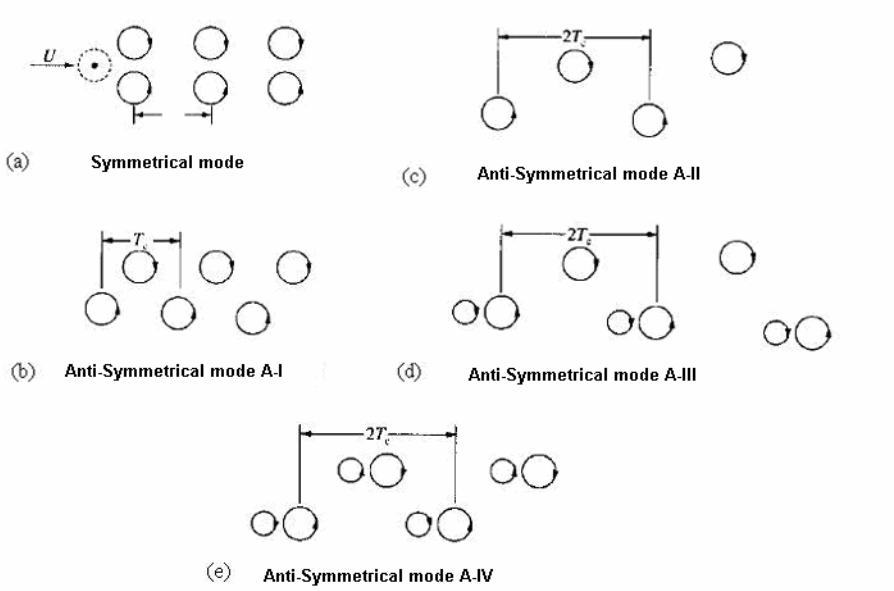

Figure 1:Modes of emission of vortices, removed from Öngoren & Rockwell (1988). (a) Symmetrical mode; (b) Anti-Symmetrical mode A-I; (c) Anti-Symmetrical mode A-II; (d) Anti-Symmetrical mode A-III; (e) Anti-Symmetrical mode A-IV; Forms of topology of wake observed by Öngoren & Rockwell (1988).

Later, Cetiner & Rockwell (2001) had carried through focused experimental study in the *Lock-on* state, or synchronization, in the formation of the vortices. This phenomenon occurs when the frequency of emission of vortices is determined primordially by the frequency of oscillation of the cylinder. They had noticed that this phenomenon occurs for the harmonic ones of the basic frequency of emission of vortices, in the case where the cylinder remains static. Additionally, some analyses of numerical simulations has been proposals for the cylinder oscillating in the direction of an incident flow, carried through for Justesen (1991) that confirms some regimes described for Tatsuno & Bearman (1990) for a static fluid; Guilmineal et. al (2002) simulating oscillations in the direction of the flow for Re=100 and KC=5, however for static flow; Song et. al (2002) that they argue a flow in the limit of the laminar flow, Re=200; beyond Dütsch et. al (1998), had confirmed numerically all regimes of flow argued by Öngoren & Rockwell (1988). Two new concepts are added to the introduction; the reduced velocity, and the reduced frequency, of the cylinder. The reduced velocity represents the rate between the maximum velocity of displacement of the cylinder by the velocity of the flow not disturbed. Therefore, if the displacement of the cylinder is a harmonic function of the type presented in Eq. 1.1:

$$x_c(t) = \frac{\mathrm{A}}{2} sin(2\pi f\ t). \tag{1.1}$$

The velocity of the cylinder is given by the first derivative of Eq. 1.1, in the form that follows:

$$\mathrm{U}_c(t) = \pi f\ \mathrm{A}\ cos(\underbrace{2\pi f\ t}_{\phi}). \tag{1.2}$$

The point of maximum of the function represented by the Eq. 1.2 occurs when $\phi = 0$, where $cos(2\pi f\ t) = cos(0) = 1$. Therefore, the reduced velocity is given by:

$$\mathrm{U}_r = \pi f\ \mathrm{A}\ . \tag{1.3}$$

The reduced frequency is defined as the rate between the oscillation frequency of the cylinder by the vortex-emission frequency in the static case, where f_c represents the oscillation frequency of the cylinder.

$$f_r = \frac{f_c}{f_0}. \tag{1.4}$$

2. Methodology

The physical formulation of the problem considers a compressible and two dimensional Newtonian fluid over a non-inertial frame. This aspect of the flow is added to the mathematical formulation as a pseudo-force in momentum equation and as a pseudo-work in the energy equation, Batchelor (2000). Therefore, the governing equations of the problem are presented in Einstein notation and non-dimensional form of its propertys as: the conservation mass, momentum and energy equations, respectively:

$$\frac{\partial \rho}{\partial t} + \frac{\partial}{\partial x_i}\left(\rho u_i\right) = 0\,; \tag{2.1}$$

$$\frac{\partial}{\partial t}\left(\rho u_i\right) + \frac{\partial}{\partial x_j}\left(\rho u_i u_j\right) = -\frac{\partial p}{\partial x_i} + \frac{\partial \tau_{ij}}{\partial x_j} + \rho f_i\,; \tag{2.2}$$

$$\frac{\partial}{\partial t}\left(\rho e_T\right) + \frac{\partial}{\partial x_i}\left(\rho e_T u_i\right) = -\frac{\partial}{\partial x_i}\left(p u_i\right) + \frac{\partial}{\partial x_i}\left(\tau_{ij} u_j\right) - \frac{\partial q_i}{\partial x_i} + \rho f_i u_i\,; \tag{2.3}$$

$$x_c(t) = \frac{\mathrm{A}}{2}\mathbf{sin}\left(2\pi f\, t\right); \tag{2.4}$$

where x_i represents the spatial cartesian coordinate in *i*-direction; ρ, the specific mass; t, temporal coordinate; *p*, the thermodynamic pressure; τ_{ij}, the viscous tensor for a Newtonian fluid; e_T, is the total energy by mass unit; u_i and u_j represents the velocity component in *i* and *j*-direction; q_i is the density heat transfer in *i*-direction; and ρf_i represents the pseudo-force in *i*-direction. This collection of equations is named as Navier-Stokes equations and is normalized as suggested by Anderson (2001). Additionally, the hypothesis of a gas caloric and thermally perfect is accepted; moreover the perfect gas state equation is used to connect the pressure and the temperature.

The pseudo-force is attached to the oscillatory movement of the circular cylinder represented by $x_c(t)$; resulting in the above equation,

$$\rho f_i = \rho \frac{\partial^2}{\partial t^2}\left[x(t)\right] = \rho 2\mathrm{A}\,(\pi f)^2\,\mathbf{sin}\left(2\pi f\, t\right). \tag{2.5}$$

where, *f* and A represents, respectively, the non-dimensional frequency of oscillation and amplitude of displacement of the cylinder.

The boundary conditions consist of imposing the non-slip condition in the solid wall of the cylinder, condition of adiabatic wall and null gradient of pressure in the normal direction to the wall, approximation of boundary layer, which implies at, respectively;

$$u_i = u_{is} \quad , \quad \frac{\partial T}{\partial n} = 0 \quad , \quad \frac{\partial p}{\partial n} = 0\,, \tag{2.6}$$

where the subscript *is* corresponds to the component of the velocity vector in the *i*-direction on the solid surface and *n* represents the normal direction to the surface.

The Eq. 2.2, 2.3, 2.4 can be written in vectorial notation as follows:

$$\frac{\partial \mathbf{U}}{\partial t} + \frac{\partial \mathbf{E}}{\partial x} + \frac{\partial \mathbf{F}}{\partial y} = \mathbf{R}\,, \tag{2.7}$$

where, **U**, represents the conservative variable vector in a non-dimensional form; **E** and **F** represents the flux vectors of the properties in a non-dimensional form; and **R** represents the source term, Anderson et al (2000), which is responsible for the pseudo-force, originated by the oscillatory displacement of the cylinder. However, the movement of the cylinder occurs only in the *x*-direction, therefore, the vector **R** results in:

$$\mathbf{R} = \begin{bmatrix} 0 \\ \rho f_x \\ 0 \\ \rho u f_x \end{bmatrix}, \tag{2.8}$$

To numerically solve the described system the explicit method of Ducros is used, the formulation uses a finite volumes approach which was demonstrated in Mendonça (2004). Then, to make the spatial discretization a flux tensor $\mathbf{\Pi}$ was defined, with the following property:

$$\nabla \cdot \mathbf{\Pi} = \frac{\partial \mathbf{E}}{\partial x} + \frac{\partial \mathbf{F}}{\partial y}. \tag{2.9}$$

Therefore, the Eq. 2.9 can be rewritten in the form that follows:

$$\frac{\partial \mathbf{U}}{\partial t} + \nabla \cdot \mathbf{\Pi} = \mathbf{R}. \tag{2.10}$$

The equation above is integrated for an arbitrary control volume $\forall$, resulting in the following equation:

$$\frac{\partial}{\partial t}\int_{\forall} \mathbf{U}\, d\forall - \int_{\forall} \nabla \cdot \mathbf{\Pi}\, d\forall + \int_{\forall} \mathbf{R}\, d\forall. \tag{2.11}$$

Thus, under the hypothesis of that the control volume is invariant with the time the divergent theorem is applied to the flux terms, transforming the integral of volume into an integral of surface, resulting in:

$$\frac{\partial}{\partial t}\int_{\forall} \mathbf{U}\, d\forall = -\int_{S} \mathbf{\Pi} \cdot \mathbf{n}\, dS + \int_{\forall} \mathbf{R}\, d\forall, \tag{2.12}$$

where $\mathbf{n}$ represents the normal vector to the surface of the control volume .

If the volumetric averages of the vectors $\mathbf{U}$ and $\mathbf{R}$ can be defined for arbitrary control volume $\forall$, the following equations are obtained:

$$\overline{\mathbf{U}} \equiv \frac{1}{\forall}\int_{\forall} \mathbf{U}\, d\forall \quad \text{e} \quad \overline{\mathbf{R}} \equiv \frac{1}{\forall}\int_{\forall} \mathbf{R}\, d\forall, \tag{2.13}$$

which, if replaced in the Eq. 2.12, results in:

$$\frac{\partial \overline{\mathbf{U}}}{\partial t} - \frac{1}{\forall}\int_{S} \mathbf{\Pi} \cdot \mathbf{n}\, dS + \overline{\mathbf{R}}. \tag{2.14}$$

For a two dimensional control volume a first order approach is realized, inducing a temporal variation of the vector U , shown in the Eq. 2.15.

$$\left(\frac{\partial \overline{\mathbf{U}}}{\partial t}\right)_{i,j} = \frac{\Delta \overline{\mathbf{U}}_{i,j}}{\Delta t} + (O)\Delta t, \tag{2.15}$$

where, $\Delta\overline{\mathbf{U}}$ represents the variation of the vector $\overline{\mathbf{U}}$ in the time step, Δt. Resulting in a temporal approach of the Eq. 2.14, which for a quadrilateral bidimensional control volume, results in:

$$\Delta\overline{\mathbf{U}} = -\frac{\Delta t}{\forall_{i,j}}\left[\int_{s_{i+1/2}} \mathbf{\Pi} \cdot \mathbf{n} dS + \int_{s_{i-1/2}} \mathbf{\Pi} \cdot \mathbf{n} dS + \int_{s_{j+1/2}} \Pi \cdot \mathbf{n} dS + \int_{s_{j-1/2}} \mathbf{\Pi} \cdot \mathbf{n} dS\right] + \Delta t\, \overline{\mathbf{R}}_{i,j}, \tag{2.16}$$

where $S_{i+1/2}, S_{i-1/2}, S_{j+1/2}, S_{i-1/2}$, represents the surfaces that define the faces of the quadrilateral, shown in Fig. 2. The sub-index represent the adjacent control volumes with which the control surfaces are shared, it means, the surface $S_{i+1/2}$ are shared by the volume (i, j) with the volume $(i+1, j)$.

However, to numerically solve the Eq. 2.16, it is necessary to approach the integrals of surface. Therefore, the consideration of the flux tensor Π is a constant in the surface S are used, as follows;

$$\int_{S} \mathbf{\Pi} \cdot \mathbf{n}\, dS \cong \mathbf{\Pi} \cdot \int_{S} \mathbf{n}\, dS = \mathbf{\Pi} \cdot \mathbf{S}, \tag{2.17}$$

where, $\mathbf{S}$ represents the surface vector associated to the surface S. The approximation is necessary because, in a finite volume formulation, only the volumetric averages of the properties are known.

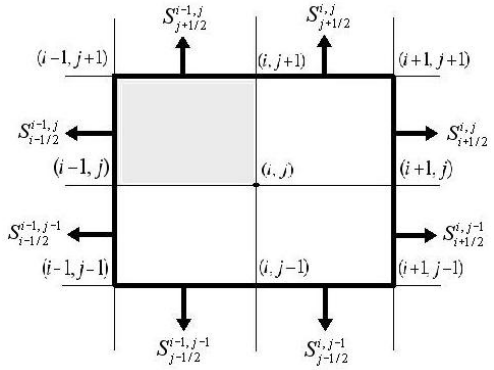

Figure 2: Control volume contend a point of the mesh for the bidimensional case with fourth order of spatial precision. The solid line of bigger thickness involves the volume around of the mesh point; the volume shading represents the discretization in finite volumes.

It is defined, then, the function of liquid flux, $F\left(\overline{\mathrm{U}}\right)_{i,j}$, of the tensor $\mathbf{\Pi}$ on the control surface, in the form;

$$F\left(\overline{\mathrm{U}}\right)_{i,j} = \frac{\Delta t}{\overline{\mathrm{V}}_{i,j}}\left[\left(\mathbf{\Pi}\cdot\mathbf{S}\right)_{i+1/2} + \left(\mathbf{\Pi}\cdot\mathbf{S}\right)_{i-1/2} + \left(\mathbf{\Pi}\cdot\mathbf{S}\right)_{j+1/2} + \left(\mathbf{\Pi}\cdot\mathbf{S}\right)_{j-1/2}\right]. \tag{2.18}$$

Then, the Eq. 2.16 can be rewritten as follows:

$$\Delta\overline{\mathrm{U}}_{i,j} = -\left[F\left(\overline{\mathrm{U}}\right)_{i,j} + D\left(\overline{\mathrm{U}}\right)_{i,j}\right] + \Delta t\,\overline{\mathrm{R}}_{i,j}, \tag{2.19}$$

where, $D\left(\overline{\mathrm{U}}\right)_{i,j}$ represents an artificial dissipation in the volume (i,j). This dissipation is explicitly imposed to stabilize the numerical method.

To carry out the temporal evolution of the Eq. 2.19, a variation of the Runge-Kutta method with a third order precision is used, proposal by Shu and described by Yee (1997), as follows:

$$\overline{\mathbf{U}}^{1} = \left[F\left(\overline{\mathbf{U}}^{n}\right) + D\left(\overline{\mathbf{U}}^{n}\right) + \Delta t\,\overline{\mathbf{R}}^{n}\right]; \tag{2.20}$$

$$\overline{\mathbf{U}}^{2} = \frac{3}{4}\overline{\mathbf{U}}^{n} + \frac{1}{4}\overline{\mathbf{U}}^{1} - \frac{1}{4}\left[F\left(\overline{\mathbf{U}}^{1}\right) + D\left(\overline{\mathbf{U}}^{1}\right) + \Delta t\,\overline{\mathbf{R}}^{1}\right]; \tag{2.21}$$

$$\overline{\mathbf{U}}^{n+1} = \frac{1}{3}\overline{\mathbf{U}}^{n} + \frac{2}{3}\overline{\mathbf{U}}^{1} - \frac{2}{3}\left[F\left(\overline{\mathbf{U}}^{2}\right) + D\left(\overline{\mathbf{U}}^{2}\right) + \Delta t\,\overline{\mathbf{R}}^{2}\right]. \tag{2.22}$$

In the previous equations, $\overline{\mathrm{U}}^{1}$ and $\overline{\mathrm{U}}^{2}$ are intermediate vectors used to the accomplishment of the calculation of $\overline{\mathrm{U}}^{n+1}$ and the respective fluxes, $F\left(\overline{\mathrm{U}}^{n}\right)$, and dissipations, $D\left(\overline{\mathrm{U}}^{n}\right)$.

The numerical simulation uses a structuralized grid with O format and resolution of 360 points in the angular direction and 315 points in the radial direction, totalizing 113400 volumes. The time-step, Δt, are determined using the criterion of entrance of Courant-Friedrichs-Lewis (CFL), Anderson et al (2000), considering the velocity of propagation of the sound. Moreover, the boundary conditions of the computational domain considers the hypothesis of that the flux of any property, ϕ, of the fluid is invariant on the surface, η_f, of the border. It means;

$$\frac{\partial\phi}{\partial\eta_f} = 0\,. \tag{2.22}$$

These conditions are used in the border of the domain because the imposition of non-disturbed properties of the flow in the computational border would cause the reflection of the waves of pressure generated by the oscillation movement of the cylinder and it would cause interference in the near region to the cylinder.

3. Results

3.1 Static Cylinder

The numerical simulation of the laminar flow around of a fixed circular cylinder, $\mathrm{Re} = 100$, was executed in order to use the output parameters, as the number of Strouhal, f_0. The following figure, Fig. 3, represents the power spectrum of the lift coefficient, where the peak indicates the dominant frequency that the alternating emission of vortices occurs and defines the number of Strouhal, $f_0 \approx 0.15$.

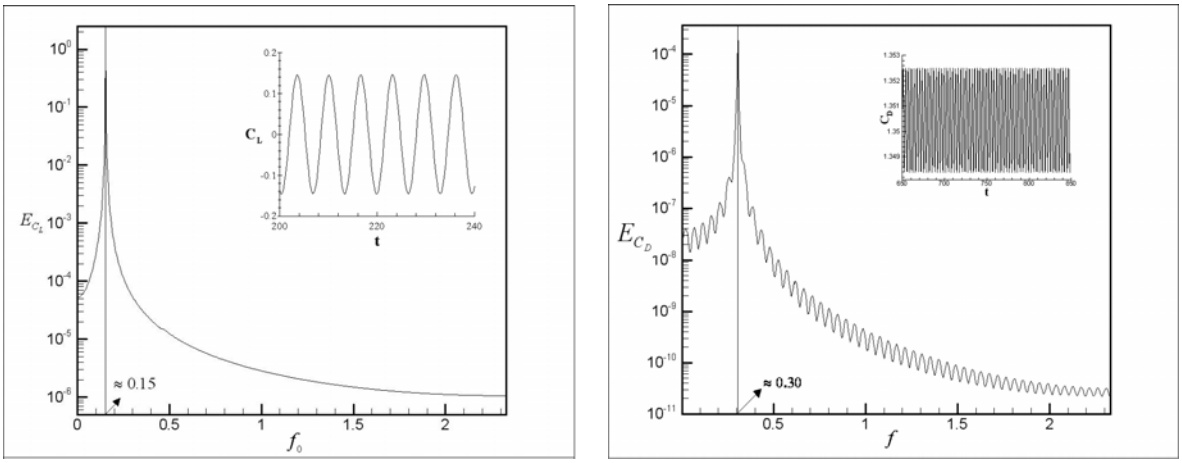

Figure 3: Power Spectrum of the lift coefficient on the left side and the drag coefficient on the right side, component that acts in the normal direction to the flow on the cylinder, Re=100. In the upper right corner the signal of the lift coefficient in function of the nondimensional time.

Can be observed from the figures that the dominant frequency of the drag coefficient it's about two times the frequency of the lift coefficient, as expected from the literature. The flow around a static cylinder presented itself steady, has emission of alternating and symmetrical vortices, characterizing the wake of the type presented by von Kármán, the Fig. 4 shows the temperature gradient visualization.

Figure 4: Temperature gradient visualization for the static cylinder at Re=100.

This type of configuration of wake is a typically defined as von Kármán wake and in this case the temporal average of the lift coefficient is null, but the r.m.s *(root mean square)* average have the value of $C_{L\,r.m.s} = 0.1033$ and in the other hand the temporal average of the drag coefficient is $C_D = 0.1033$. The power spectra of the output were obtained applying to the output a FFT *(Fast Fourier Transform)*.

3.2 Oscillatory Cylinder

In the hypothesis of the cylinder oscillating in-line with the flow, some simulations with different configurations of reduced velocity, reduced frequency and non-dimensional amplitude are proposals. The purpose of these simulations is topologically group the possible types of wake, inside of the executed simulations, using as analysis tool the generated graphs, from the output signals of the lift and the drag coefficient, and the visualization of the temperature gradient. Leaving of this premise, are presented the data of the simulations executed for the different configurations of the considered flow, varying the reduced velocity and the reduced frequency.

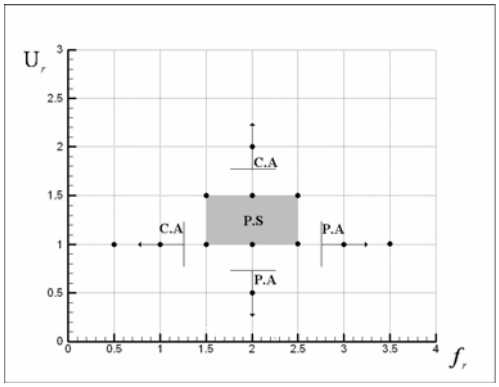

Figure 5: Demonstrative of executed simulation.

The graphic of the Fig. 5 shows the executed simulations on this work, the shading part of the graphic means the periodic symmetrical region, P.S; C.A means chaotic anti-symmetrical; and P.A means periodic anti-symmetrical. These symbols represent the topology of wake found in this present work and shows its tendency to become.

3.2.1 Periodic Symmetrical

In this configuration of the flow, pairs of vortices are emitted to each cycle of oscillation of the cylinder, having become the flow completely symmetrical. The consequence of this symmetry reflects in the extinguishing of the component of normal force on the cylinder, lift force, only acting the in-line component with the flow. This characteristic of the flow is the greater point and importance of the present study, once to certain parameters a component of force that normally would act on the system is annulled.

The emission dynamics of vortices can be described in the following way: In accordance with the movement of the cylinder in the negative direction of the oscillation axle, a zone of recirculation in the boundary layers in the upper and lower side of the cylinder is formed, which separates in the same place above and in a low position of the surface of the cylinder, Fig. 6(a); it forms then two zones of recirculation of same intensity and size, resulting in a same format downstream of the cylinder, Fig. 6(b); however, with appositive rotation. The increase of this zone of recirculation arrives to the end when the cylinder reaches the position $_{-A/2}$, position in which is initiated the contrary movement of displacement, positive direction in relation to the oscillation axle, Fig. 6(c); as the cylinder covers the positive direction, a new boundary layer is generated, must be noticed that if it didn't have an incident flow the formation of the vortices would be that described by Tatsuno & Bearman (1990), however, the incident flow functions as a barrier to the formation of these "opposite vortices" in relation to the vortices of bigger intensity, confining them as seemed in the Fig. 6(d); additionally, the emission of the pairs of vortices occurs when it has the inversion of the movement from the point of maximum of the displacement of the cylinder, Fig. 6(e).

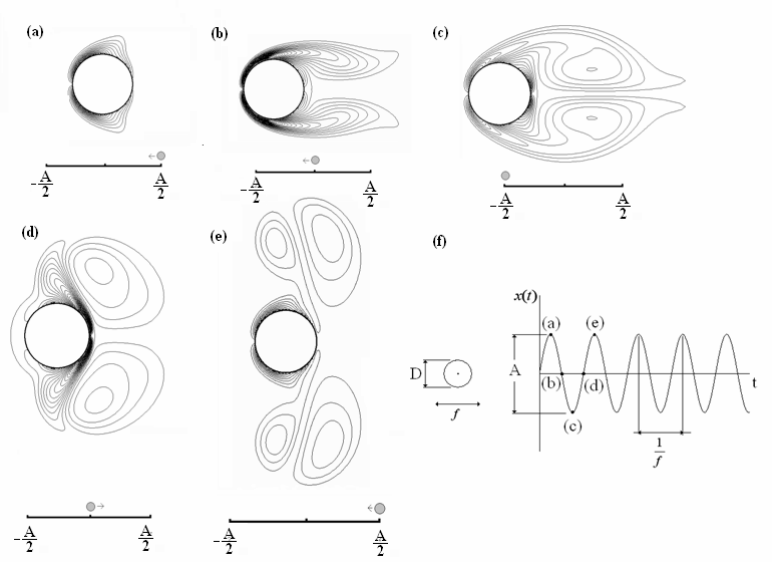

Figure 6 : Visualization of vorticity iso-lines, for: $\theta = 2\pi f_c \cdot t$; (a) $\theta \approx 90°$, (b) $\theta \approx 180°$, (c) $\theta \approx 270°$, (d) $\theta \approx 360°$, (e) $\theta \approx 450°$.

The following figures show the temperature gradient visualization for the shading region of the graphic of Fig. 5.

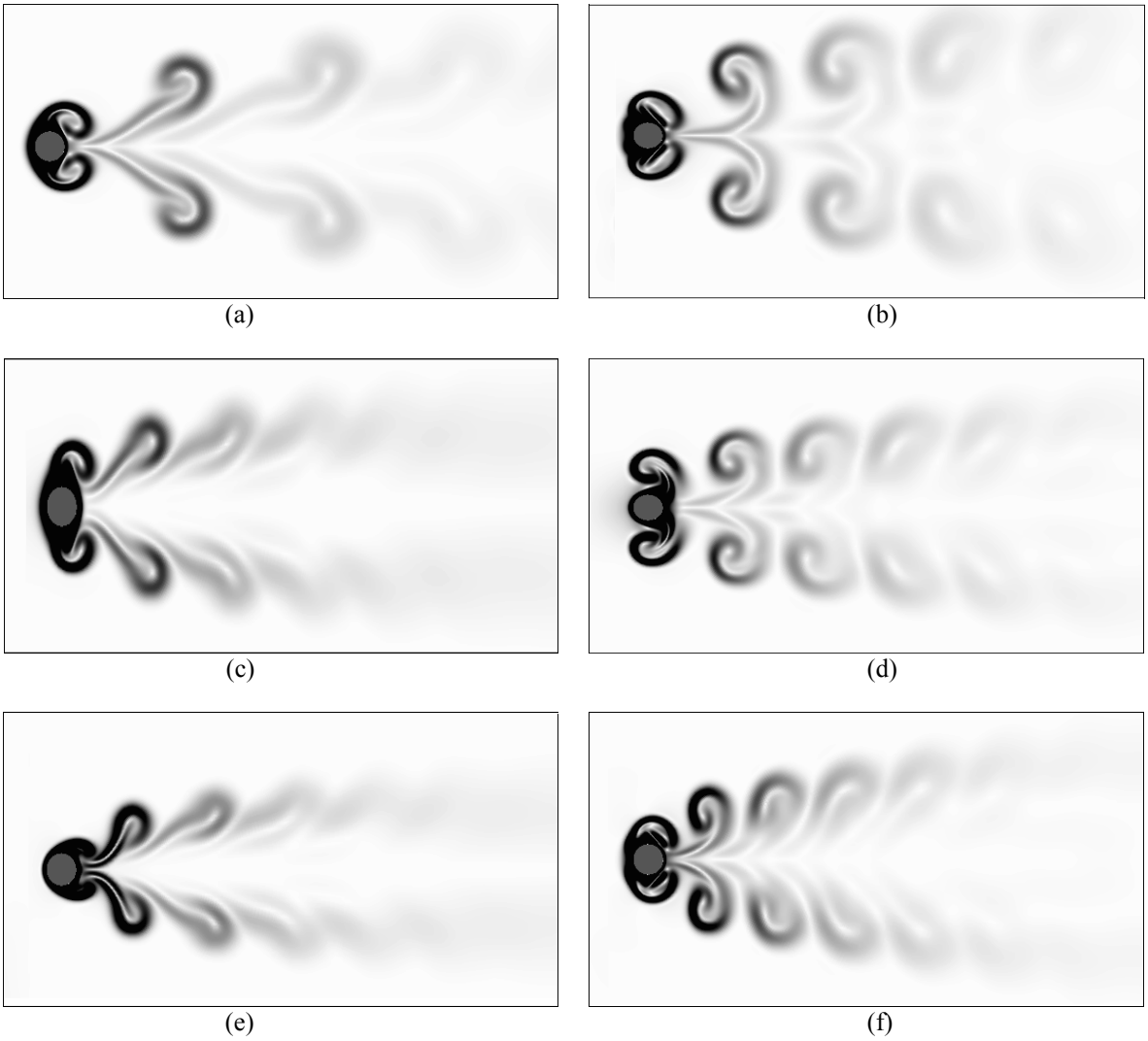

(a) (b) (c) (d) (e) (f)

Figure 7: Temperature gradient visualization, (a) U_r=1.0 and f_r=1.5; (b) U_r=1.5 and f_r=1.5; (c) U_r=1.0 and f_r=2.0; (d)U_r=1.5 and f_r=2.0; (e) U_r=1.0 and f_r=2.5; (f) U_r=1.5 and f_r=2.5.

The following figures illustrate the power spectrum of the drag coefficient;

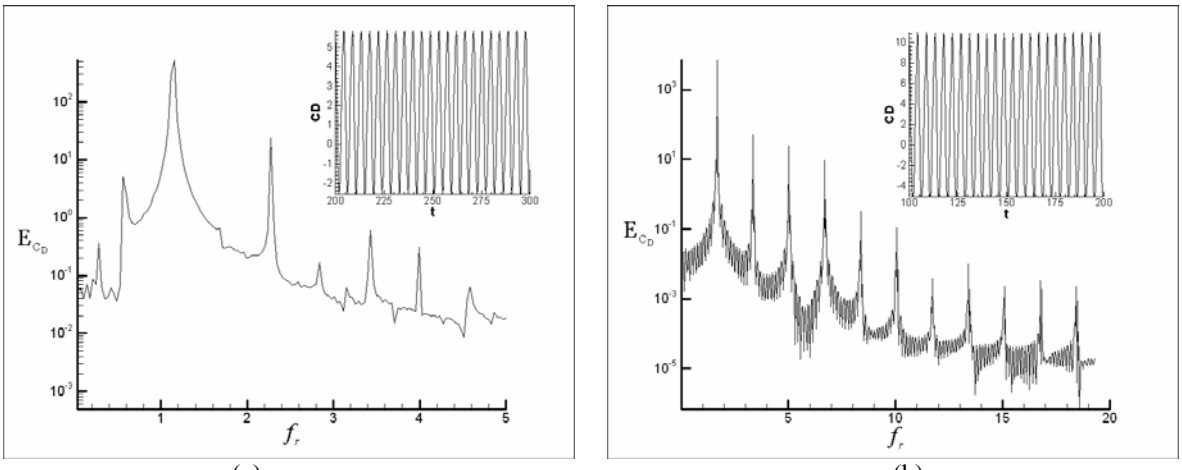

(a) (b)

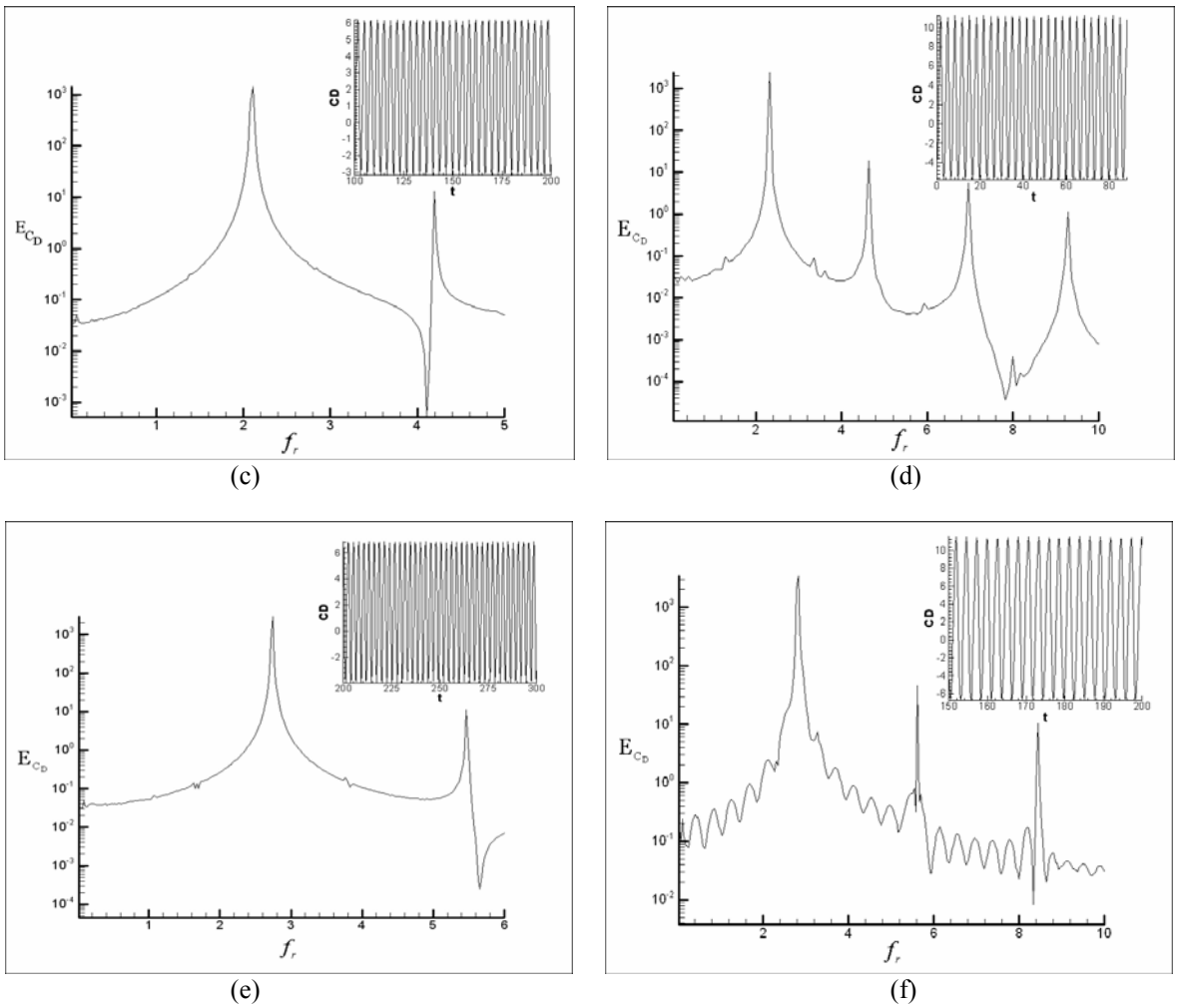

Figure 10: Power spectrum of the drag coefficient, (a) U_r=1.0 and f_r=1.5; (b) U_r=1.5 and f_r=1.5; (c) U_r=1.0 and f_r=2.0; (d) U_r=1.5 and f_r=2.0; (e) U_r=1.0 and f_r=2.5; (f) U_r=1.5 and f_r=2.5.

In this case all the dominant frequencies showed by power spectrum are harmonics of the frequency of excitation of the system. The analysis of the signal of lift coefficient was omitted because

3.2.2 Periodic Anti-Symmetrical

This configuration of the flow presents an interesting characteristic, in the near region of the cylinder the wake has similar topology to P.S mode, periodic symmetrical. However, the vortices generated by the displacement of the cylinder combine themselves for form a vortex of bigger intensity and that will give beginning to a wake with typical characteristic of the von Kármán wake. Composing itself by two distinct regions: the first one near to the cylinder that shares characteristics with P.S mode; and the other region away from the cylinder that has the characteristic of the von Kármán vortices, however the disturbance that provokes the decline for P.A mode, has origin in a region away from the cylinder, dislocating itself from the downstream of the wake until the near region to the cylinder inducing, then, the coalescence of the vortices and forming the described topology, as exposed in the following graphics of Fig. 9.

The disturbance that support the decline to P.A mode evolve temporarily in the downstream direction of the flow, from a distant point of the cylinder, $L >> D$. The vorticity field grows with the time and that increase of magnitude that initially forms a great steady region of vorticity with opposite rotational direction, although for some reason the whole structure comes down because the disturbance travels in the downstream direction and when it approaches to the region of influence of the cylinder, near wake region, occurs the rupture of this zone of recirculation and consequence of that is the emission of vortices.

By the power spectrum can be seem that the output signals of the system with the excitation of the cylinder has many frequencies as response for principal excitation of the cylinder, producing a highly modulated signal.

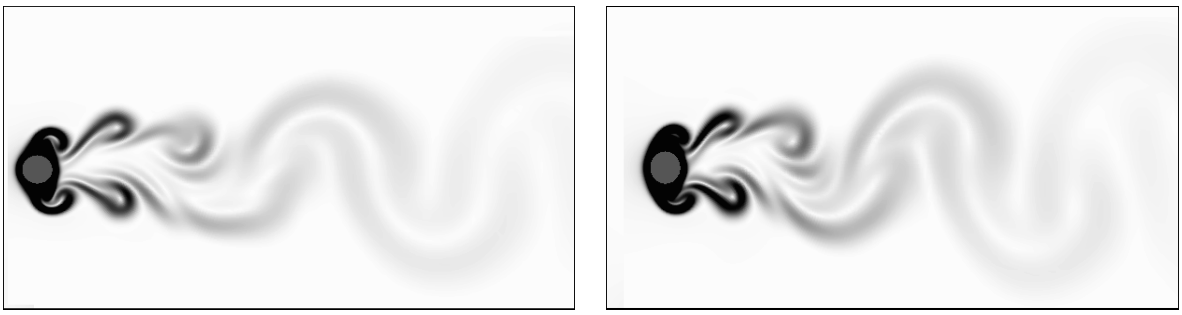

(a) (b)

Figure 9: Temperature gradient visualization, (a) U_r=1.0 and f_r=3.0; (b) U_r=1.0 and f_r=3.5

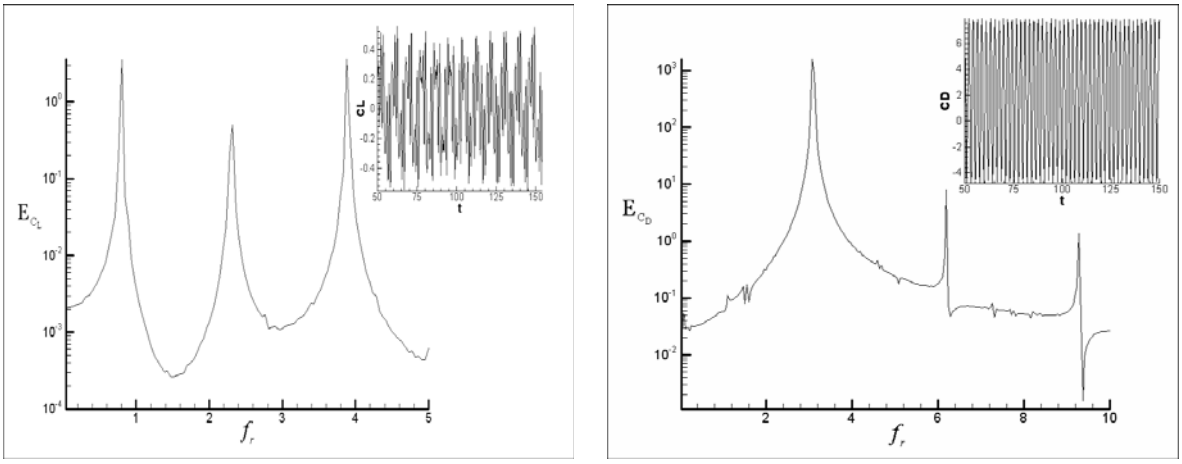

(a) (b)

Figure 10: Power spectrum of the output signals for U_r=1.0 and f_r=3.0.

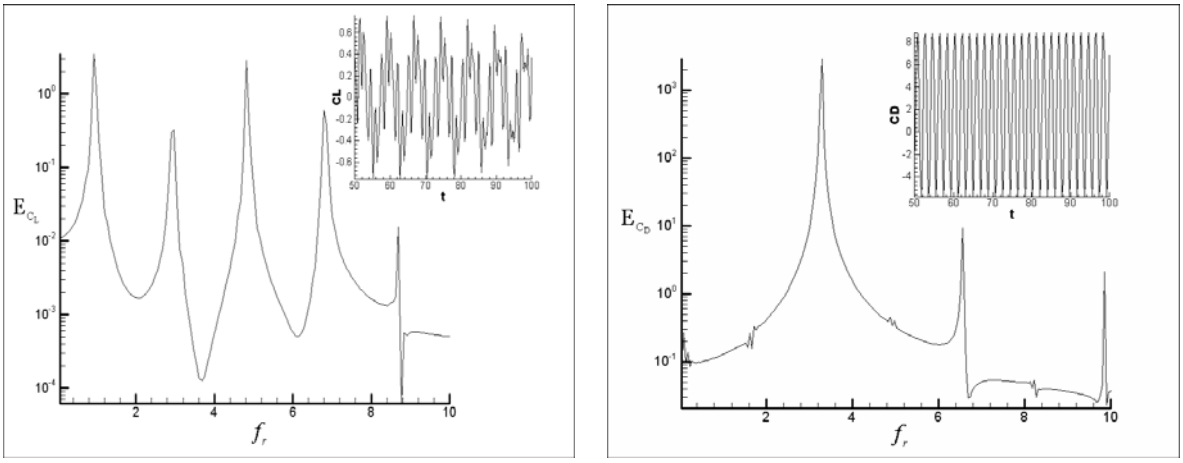

(a) (b)

Figure 11: Power spectrum of the output signals for U_r=1.0 and f_r=3.5; (a) lift and (b) drag coefficient.

3.2.3 Chaotic Anti-Symmetrical

In this flow configuration the vortices are generated and emitted aleatorily without any synchrony or regularity, and in which the interaction mechanism between the vortices, cylinder and flow is extremely complex and a non linear configuration, the disturbance that induces the decline for C.A mode has origin in the near wake region to the cylinder, the Fig. 12, as show below that illustrate two visualizations of this chaotic regime;

The Fig. 15 explains the time average values of the lift and drag coefficient for comparison.

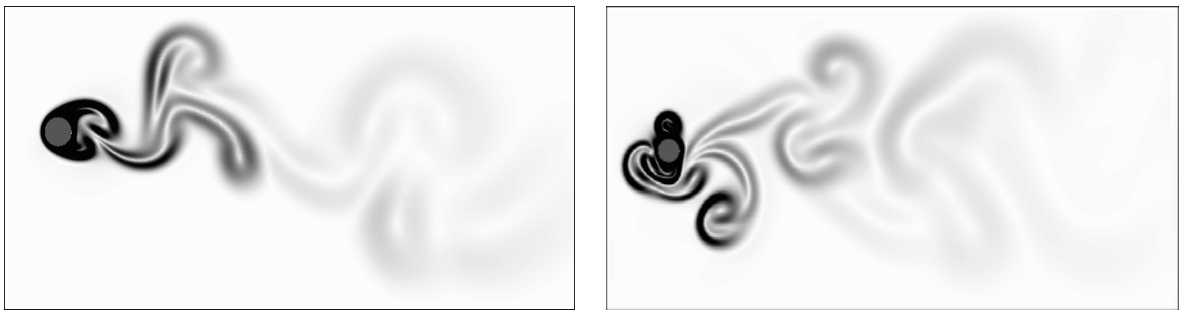

(a) (b)

Figure 12: Temperature gradient visualization, (a) U_r=1.0 and f_r=0.5; (b) U_r=2.0 and f_r=2.0

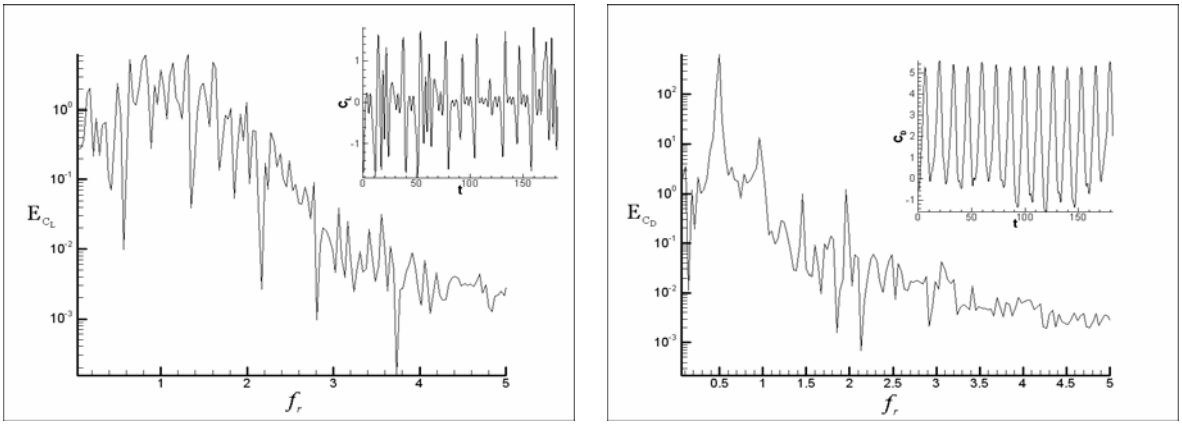

(a) (b)

Figure 13: Power spectrum of the output signals for U_r=1.0 and f_r=0.5; (a) lift and (b) drag coefficient.

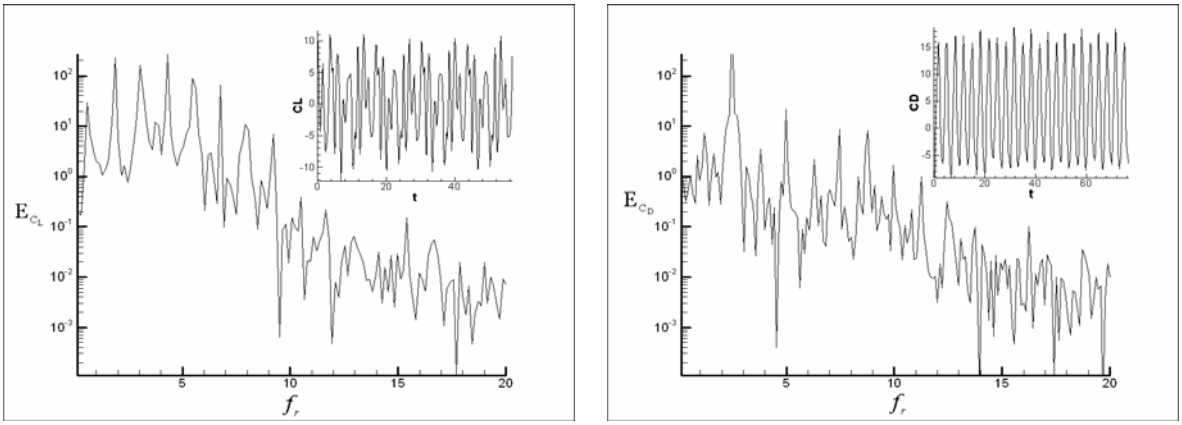

(a) (b)

Figure 14: Power spectrum of the output signals for U_r=2.0 and f_r=2.0; (a) lift and (b) drag coefficient.

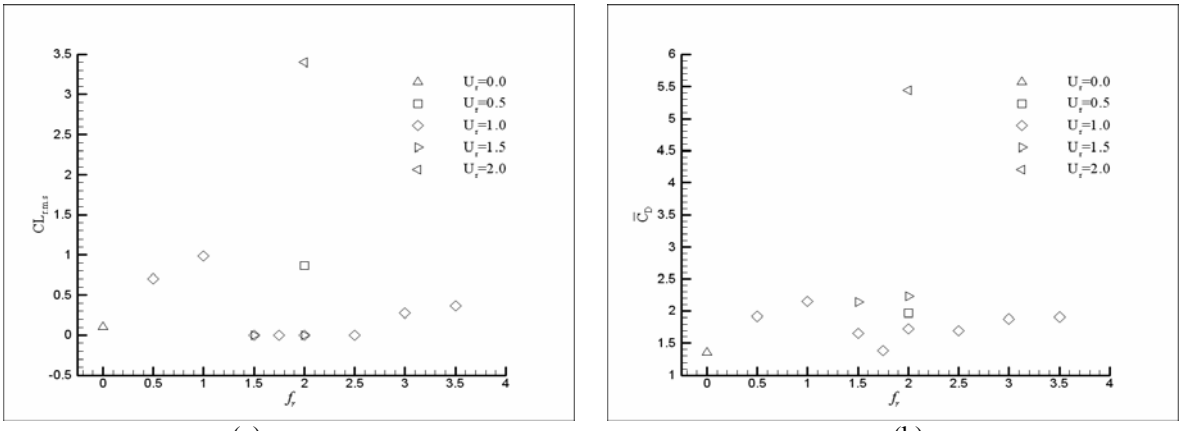

(a) (b)

Figure 15: The temporal averages of the output coefficient; (a) lift (r.m.s) and (b) drag coefficient.

4. Conclusions

The present study had as main proposal, the topological analysis of a laminar flow around a circular cylinder with streamwise oscillation, through the analysis of the data of the numerical simulations. Ahead on this, it was observed the existence of three main and distinct ways of topology: the main way is called periodic symmetrical, P.S, where the symmetry in relation to the x-axle promotes the extinguishing of the normal component of operating force on the cylinder, without affect or increases the magnitude of in-line component acting on the cylinder, its main characteristic, in P.S mode, is the emission of pairs of vortices in each cycle of oscillation of the cylinder. The secondary ways are characterized by the decline of P.S mode to: chaotic anti-symmetrical, C.A; and periodic anti-symmetrical, P.A, modes.

In the secondary mode, C.A, the characteristics of the flow are chaotic anti-symmetrical, this means that the topology of the wake doesn't present a permanent configuration, throughout the time, additionally in this mode the component of normal force to the flow, doesn't present a null temporal average. in the secondary mode, P.A, the wake are divided in two regions, the first one near to the cylinder which has similar characteristics with the mode P.S, and other region away from the cylinder, in the wake, and that have topology of the type von Kármán.

On this work was found some possible topology wake, becoming it successful in its initial proposal. However, could be possible that other configurations of the parameters reduced velocity and reduced frequency may promote the sprouting of other types of wake topology, once that the literature on the subject mentions endless configurations for the wake topology.

5. References

ANAGNOSTOPOULOS, P. & ILIADIS, G., "Numerical study of the flow pattern an the in-line respose of a flexible cyrcular cylinder in an oscillating stream", J. Fluid and Structures (1998), vol. 12, pp. 225-258.

ANDERSON, D. A., TANNEHILL, J. C. & PLETCHER, R., "Computational Fluid Mechanics and Heat Transfer", Hemisphere Publishing Company, New York, 2000.

ANDERSON, J. D., Jr., "Fundamentals of Aerodynamics", McGraw-Hill Higher, Education, 2001, p.p. 15-21.

BATCHELOR, C. K, "An Introdution to Fluid Dynamics", University Press, Cambridge (2000).

BLACKBURN, H. M. & HENDERSON R. D., "A study of two-dimensional flow past an oscillating cylinder", J. Fluid and Structures (1999), vol. 385, pp. 255-286.

CENTINER, O. & ROCKWELL, D., "Streamwise oscillations of a circular cylinder in a steady current. Part 1. Loked-on states of vortex formation and loading.", L. Fluid Mech (2001), vol, 427, pp. 1-28.

GOVARDHAN, R. & WILLIAMSON C. H. K, "Modes of vortex formation and frequency response os a freely vibrating cylinder", J. Flui Mech. (2000), vol. 420, pp. 85-130.

GRIFFIN, O. M. & RAMBERG, S. E., "Vortex shedding from a cylinder vibrating in line with an incident uniform flow", J. Fluid Mech. (1976), Vol. 75, pp. 257-271.

GUIMINEAU, E. & QUEUTEY, P, "A numerical simulation of vortex shedding from na oscillaing circular cylinder", J. Fluid and Structures (2002), vol. 16(6), pp. 773-794.

H. DÜTSCH, F. DURST, S. BECKER & H. LIENHART, "Low-Reynolds-number flow around an oscillating circular cylinder at low Keulegan-Carpeter number", J. Fluid Mech (1998), vol. 360, pp. 249-271.

JUSTESEN, P., "A numerical study of oscillating flow around a circular cylinder", J. Fluid Mech (1991), vol. 222, pp. 157-196.

MENDONÇA, A. F. "Simulação Numérica do Escoamento Laminar em uma Base Bidimensional. Dissertação de Mestrado em Engenharia Mecânica, Publicação ENM.DM-081A-04, Departamento de Engenharia Mecânica, Universidade de Brasília, Brasília, DF, 143p. ano (2004).

NOBARI, M. R. H & NADERAN, H., "A numerical study of flow past a cylinder with cross and inline oscillation", Computers & Fluids (2005), pp. 1-14.

ÖNGOREN, A. & ROCKWELL, D., "Flow structure from an oscillating cylinder. Part 2. Mode competition in the near wake", J. Fluid Mech (1988), vol. 191, pp. 225-245.

TATSUNO, M & BEARMAN, "A visual study of the flow around na oscillating circular cylinder at low Keulegan-Carpenter number and low Stokes number",

ZDRAVKOVICH, M. M., " Diferent modes of vorex shedding: an overview", J. Fluid and Structrures (1996), vol. 10, pp. 427-437.